NASA Technical Memorandum 4133

A Nonlinear High Temperature Fracture Mechanics Basis for Strainrange Partitioning

Takayuki Kitamura and Gary R. Halford

OCTOBER 1989

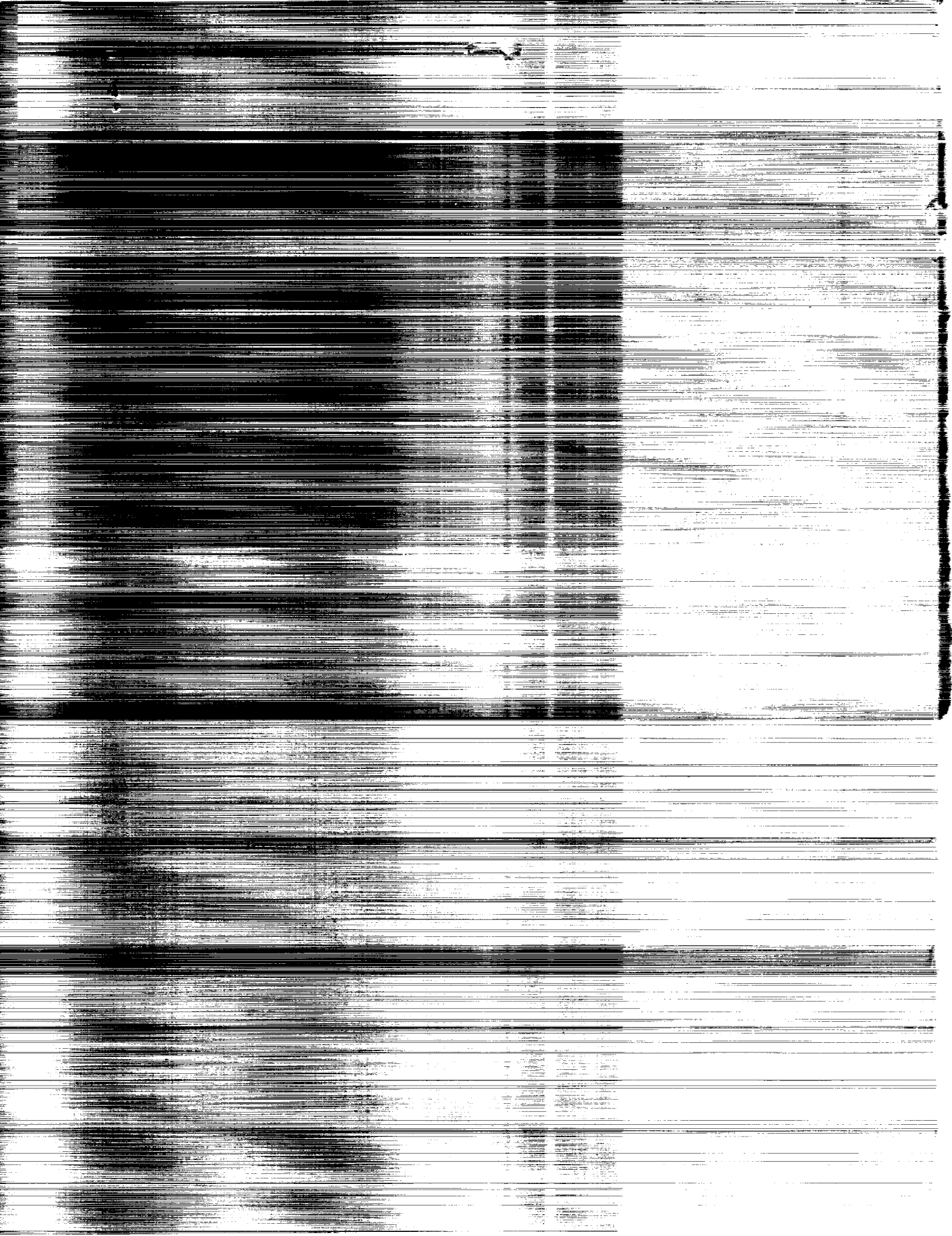

NASA Technical Memorandum 4133

A Nonlinear High Temperature Fracture Mechanics Basis for Strainrange Partitioning

Takayuki Kitamura and Gary R. Halford
Lewis Research Center
Cleveland, Ohio

National Aeronautics and
Space Administration
Office of Management
Scientific and Technical
Information Division

1989

Summary

A direct link has been established between Strainrange Partitioning (SRP) and high-temperature fracture mechanics by deriving the general SRP inelastic strain range versus cyclic life relationships from high-temperature, nonlinear, fracture mechanics considerations. The derived SRP life relationships are in reasonable agreement based on the experience of the SRP behavior of many high-temperature alloys. In addition, fracture mechanics has served as a basis for derivation of the Ductility-Normalized SRP life equations, as well as for examination of SRP relations that are applicable to thermal fatigue life prediction. Areas of additional links between nonlinear fracture mechanics and SRP have been identified for future exploration. These include effects of multiaxiality as well as low-strain, nominally elastic, long-life creep-fatigue interaction.

Introduction

At high temperatures, fatigue life prediction of structural components is much more complex than at room temperature because of deleterious time-dependent phenomena such as creep and environmental interactions. Many investigators (refs. 1 to 4) have studied the nonlinear interactions among fatigue, creep, and oxidation in this regime.

Manson and his coworkers (ref. 5) proposed the Strainrange Partitioning (SRP) method for creep-fatigue life analysis in the early 1970's. The method has seen extensive experimental evaluation (ref. 6) and its validity has been recognized in both the United States (ref. 7) and overseas (refs. 8 and 9). Application of SRP to structural components also has been pursued (ref. 10). The loading and temperature histories of an actual component, however, are complex and fatigue life is sensitive to the particular type of material and to the exact operating conditions. The SRP method of reference 5 has been improved to account for these more realistic complex conditions such as multiaxial loadings (refs. 11 and 12), cumulative damage (ref. 13), thermal fatigue (refs. 14 and 15), nominally-elastic, low-strain fatigue (refs. 16 and 17), and long-time exposure effects (refs. 18 and 19). The unified total strain version of references 20 and 21 was proposed to assist designers in applying SRP to practical engineering problems.

Fatigue crack initiation and propagation at high temperature is brought about by a variety of mechanisms including grain boundary sliding, cavity growth, crystallographic slip-plane sliding, and others (refs. 22 and 23). The failure process strongly depends on the material and the fatigue conditions in low-cycle fatigue. Under relatively high stress and strain conditions it is well established (ref. 24) that numerous small cracks initiate at a very early stage in life and thus multiple crack propagation can dominate the fatigue life. On the other hand, at lower stress and strain levels, cracks initiate considerably later in life and a single crack tends to dominate the propagation phase. Crack propagation behavior for long cracks in high temperature fatigue has been studied successfully by using nonlinear fracture mechanics (refs. 25 and 26). The effect of stress and strain waveform, cycle frequency, temperature, environment, and others have been systematically investigated on the basis of a J-integral concept by Kitamura et al. (refs. 25 and 26). High-temperature fatigue lives have been correlated to within factors of two by using these nonlinear fracture mechanics life prediction techniques. These studies have been performed independently of SRP life analysis. Since either approach provides a reasonable representation of fatigue life, it is suggested that there may well be a connection between SRP and the crack propagation relationships of nonlinear fracture mechanics.

In this study, some versions of SRP life equations are derived from previously proposed high-temperature, nonlinear, fracture mechanics formulations. This provides additional physical bases for SRP as well as a better understanding of high-temperature fatigue failure.

Fracture Mechanics Formulations at High Temperatures

Figure 1 shows the basic stress and strain waveforms and their hysteresis loops in the SRP method (refs. 2 and 27). In the SRP concept, inelastic strain is "partitioned", or divided, into time-independent plastic strain (denoted by P) and time-dependent creep strain (denoted by C). Considering the loading direction (tension and compression), fatigue at high temperature is classified into four types. The basic creep-fatigue cycle types (waveforms) shown in figure 1(a) to (d) are called PP, PC, CC, and CP fatigue, respectively. All creep-fatigue conditions are composed of these basic components.

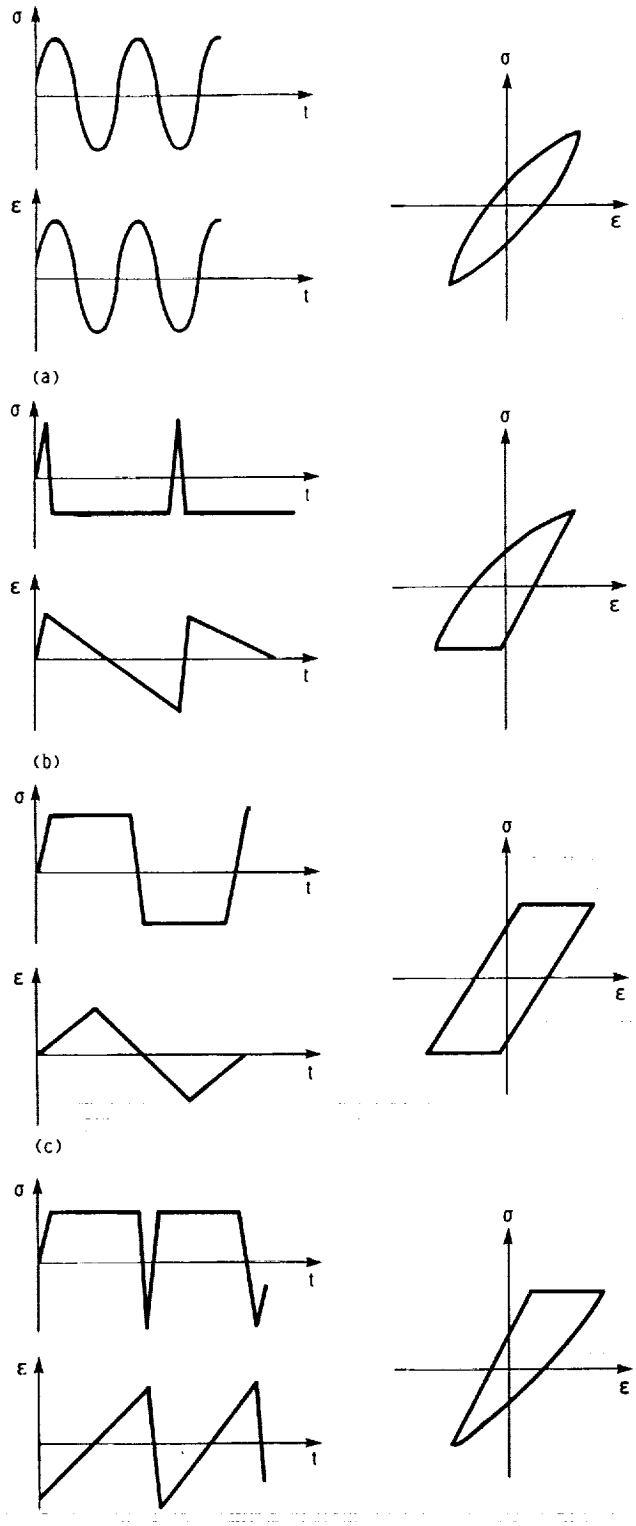

(a) PP fatigue.
(b) PC fatigue.
(c) CC fatigue.
(d) CP fatigue.

Figure 1.—Basic stress (strain) waveforms and their hysteresis loops in the SRP method.

Kitamura (refs. 25 and 26) has investigated crack propagation behavior under these basic fatigue conditions at high temperature by using nonlinear fracture mechanics. These results can be summarized as follows:

PP Fatigue

Crack propagation behavior under PP fatigue is similar to that of room temperature fatigue. The crack propagation rate, $d\ell/dN$, correlates well with the fatigue (time-independent) J-integral range (cyclic J integral (ref. 28)), ΔJ_f. The relation is of the form

$$\frac{d\ell}{dN} = C_f \Delta J_f^{m_f} \tag{1}$$

except near the threshold regime where the power law form breaks down. Here, C_f and m_f are material constants.

PC Fatigue

Compressive creep deformation has not been observed to appreciably alter the crack propagation mechanism observed during PP fatigue. Thus, the crack propagation behavior for PC fatigue is expected to obey the same form as it does for PP fatigue (eq. (1)).

CP Fatigue

Crack propagation under CP fatigue exhibits time-dependency for many materials. The time rate of crack propagation $d\ell/dt$ is nearly proportional to J^*, the creep J integral (refs. 25 and 26) (C^*-parameter (refs. 29 and 30) or modified J integral (ref. 31)), for high-temperature alloys:

$$\frac{d\ell}{dt} = C_C J^* \tag{2}$$

where C_C is the proportionality constant. The term J^* is defined as a modification of the Rice J integral, in which strain and displacement are replaced by their respective time rates of change. The term J^* uniquely characterizes the stress and strain rate field for materials following power law creep behavior.

By integrating equation (2) during the tension portion of a cycle, the time-based crack propagation equation is converted into a cycle-based equation

$$\frac{d\ell}{dN} = C_C \Delta J_C \tag{3}$$

where

$$\Delta J_C = \int_0^{t_0} J^* \, dt \tag{4}$$

and ΔJ_C is the range of the interval of creep J integral (refs. 25 and 26) and t_0 is the increasing portion of the tensile loading period of the cycle.

CC Fatigue

Compressive creep deformation added to CP fatigue can significantly alter the tensile stress-tensile creep response. In so doing, the J integral is altered along with the crack propagation rate. However, the mechanisms of CC-fatigue crack propagation remain similar to CP fatigue, and hence the form of the expression governing the propagation rates of CC fatigue is the same as for CP fatigue. Figure 2 illustrates this behavior schematically, where in figure 2(c) is a consequence of the combination of the results shown in figure 2(a) and (b).

Life Relations of Smooth Specimens

Crack Initiation and Propagation Life

In the fatigue of smooth specimens, both crack initiation life N_i and propagation life N_P contribute to the total life N_f as follows:

$$N_f = N_i + N_P = N_P(1 + \alpha) \tag{5}$$

where

$$\alpha = \frac{N_i}{N_P} \tag{6}$$

The ratio α is usually smaller than unity in low-cycle fatigue while it is larger in high-cycle fatigue. In this report only the former case is discussed. For cracks longer than a characteristic crack length ℓ_0 the fracture mechanics relations, equation (1) and (2), are applicable, while for shorter lengths, other relations must be investigated (ref. 24). In this report, we define the crack initiation life as the number of loading cycles until the crack length reaches ℓ_0. It was reported by Ohtani et al. (ref. 24), for example, that $\ell_0 = 0.1$ mm in low-cycle fatigue at 923 K for stainless steel with a 0.04 mm average grain diameter. Thus, $\ell_0 \cong 2$ to 3 grain diameters.

Crack Propagation Life in PP and PC Fatigue

The following assumptions are made for the derivation of crack propagation life:

(1) The crack propagation rates are governed by ΔJ_f as shown in equation (1).

(2) The crack length is small compared with the specimen dimensions.

(3) The relation between stress range $\Delta\sigma$ and plastic strain range $\Delta\epsilon_P$ (i.e., the cyclic stress-strain relation) is written in the form

$$\Delta\epsilon_P = A\ \Delta\sigma^{n'} \tag{7}$$

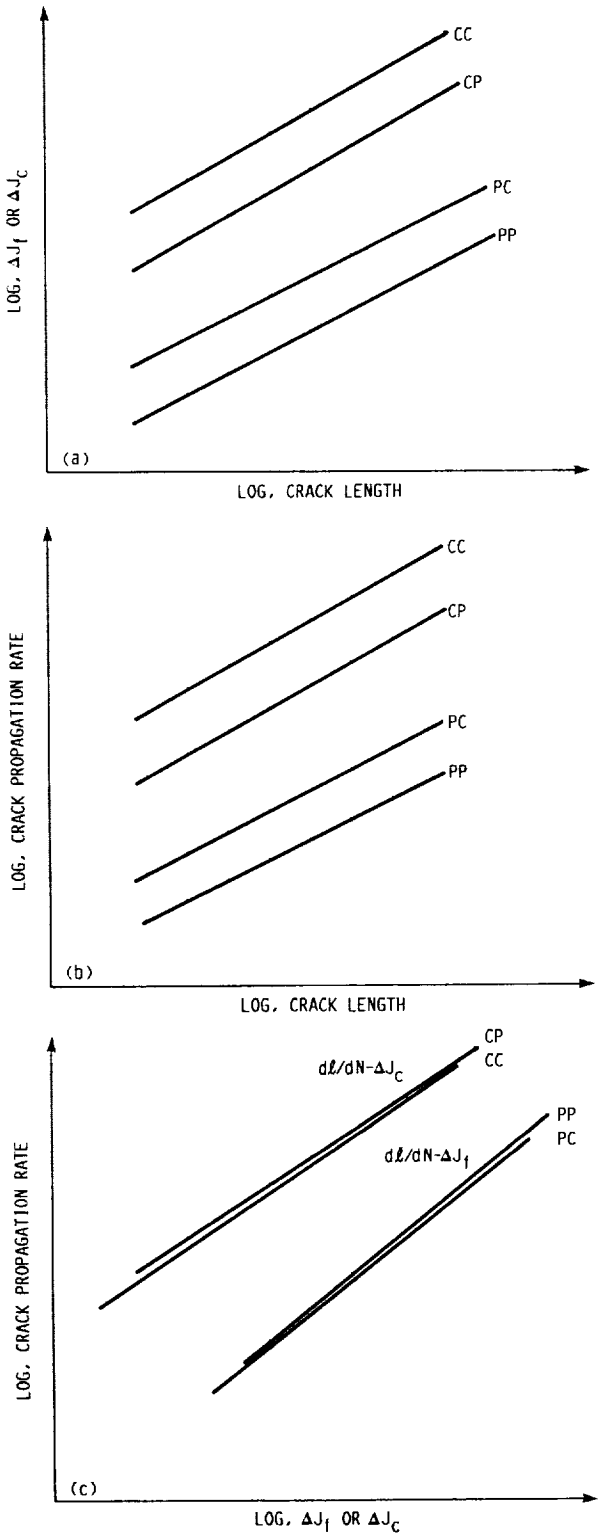

(a) J integrals as a function of crack length.
(b) Crack propagation rate as a function of crack length.
(c) Crack propagation rate as a function of J integrals for fatigue and creep.

Figure 2.—Schematic diagram explaining the effect of compressive strain on $d\ell/dN$ and the J integrals.

where A and n' are material constants.

(4) The crack tip never closes during the fatigue cycle. Assumption (4) is reasonable for short cracks in low-cycle fatigue, while the closure at the crack tip should be taken into account in high-cycle fatigue.

The fatigue J-integral range for a crack in an infinite body is the sum of elastic and plastic terms evaluated by the following (ref. 25):

$$\Delta J_f = \Delta J_e + \Delta J_P = M_J\, \Delta\sigma \ell [\pi \Delta \epsilon_e + f(n')\Delta \epsilon_P] \tag{8}$$

where M_J is a boundary-crack shape correction factor, and $f(n')$ is a function of n'. For a semicircular surface crack, they are given as follows (ref. 25):

$$M_J = 0.506 \tag{9}$$

$$f(n') = 3.85\sqrt{n'}\left(1 - \frac{1}{n'}\right) + \frac{\pi}{n'} \tag{10}$$

Dowling (ref. 32), using a different approach, derived an alternate J-integral value for the semicircular crack based on the analysis of reference 33 for a penny-shaped crack. It has a form similar to equation (8). Therefore, equations (8) to (10) will be used in this report.

Integrating equation (1) from an initial crack length ℓ_0 to a final crack length ℓ_f the following relation is derived:

$$N_P\, \Delta \widetilde{W}_f^{m_f} = D_f \tag{11}$$

$$\Delta \widetilde{W}_f = \frac{\Delta\sigma\, \Delta\epsilon_e}{2} + \left[\frac{f(n')}{2\pi}\right] \Delta\sigma\, \Delta\epsilon_P \tag{12}$$

where $\Delta \widetilde{W}_f$ is a strain energy parameter, and D_f is a parameter that is of the form

$$D_f = \frac{\ln(\ell_f/\ell_0)}{2\pi C_f M_J} \quad (m_f = 1) \tag{13a}$$

or

$$D_f = \frac{\ell_0^{1-m_f} - \ell_f^{1-m_f}}{C_f(m_f - 1)(2\pi M_J)^{m_f}} \quad (m_f \neq 1) \tag{13b}$$

A similar life relation was derived for room temperature fatigue by Mowbray (ref. 34).

Crack Propagation Life in CP and CC Fatigue

The assumptions for the derivation are as follows:

(1) Crack propagation obeys equations (2) or (3).

(2) Crack length is small compared to specimen dimensions.

(3) The relation between stress σ and creep strain rate $\dot{\epsilon}_C$ is

$$\dot{\epsilon}_C = B\sigma^n \tag{14}$$

where B and n are temperature-dependent constants.

(4) Stress waveform in tension can be approximated as shown in figure 3 and it is formulated as

$$\sigma = \sigma_{\max}\left(\frac{t}{t_0}\right)^{\beta} \tag{15}$$

where $\sigma_{\max}$ is the maximum stress, t is the time, t_0 is the tensile period, and β is a constant. Use of equation (15) is arbitrary. Other representations of the stress-time waveform could be incorporated without altering the concepts employed.

Equation (14), while based on steady state creep, can be justified for use in cycles with transient creep based on the work of Ohtani (ref. 35). He showed from a dimensionless analysis that either transient or steady state creep could be reduced to the same final result for purposes of evaluating the interval of creep J integral.

The creep J integral for a through crack in an infinite body is evaluated by the following equation (refs. 25 and 36):

$$J^* = (1 + 2\beta n) M_J \left[\frac{\sigma^2 \pi \ell}{E(n+1)t}\right] + M_J f(n) \sigma \dot{\epsilon}_C \ell \tag{16}$$

Substituting equations (14) to (16) into (4), the creep J-integral range per cycle is given by

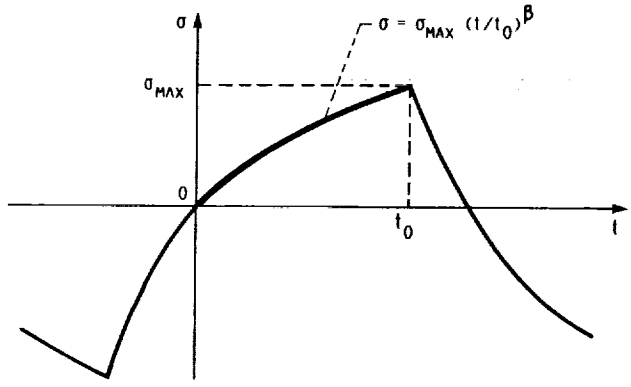

Figure 3.—Schematic diagram of stress-time relation.

$$\Delta J_C = \left[\frac{n + \left(\frac{1}{2\beta}\right)}{n+1}\right] M_J \pi \ell \left(\frac{\sigma_{max}^2}{\Delta\sigma}\right) \Delta\epsilon_e$$

$$+ \left[\frac{n\beta + 1}{(n+1)\beta + 1}\right] M_J f(n) \sigma_{max}\, \Delta\epsilon_C \ell \qquad (17)$$

The following crack propagation life relation is derived by integrating equation (3) by using equation (17):

$$N_P\, \Delta\widetilde{W}_C = D_C \qquad (18)$$

$$\Delta\widetilde{W}_C = \left[\frac{n + \left(\frac{1}{2\beta}\right)}{n+1}\right] \left[\frac{\sigma_{max}^2}{2\,\Delta\sigma}\right] \Delta\epsilon_e$$

$$+ \left[\frac{n\beta + 1}{(n+1)\beta + 1}\right] \left[\frac{f(n)}{2\pi}\right] \sigma_{max}\, \Delta\epsilon_C \qquad (19)$$

$$D_C = \frac{\ln(\ell_f/\ell_0)}{C_C 2\pi M_J} \qquad (20)$$

The solid lines in figure 4 show the upper and lower bounds of $[n + (1/2\beta)]/(n+1)$ and $(n\beta + 1)/[(n+1)\beta + 1]$ in the range of $0.3 \le \beta \le 1.0$, which corresponds with usual values for strain-controlled CP- and CC-fatigue results. The dotted curves in the figure show unity and $(n+2)/(n+3)$. It is clear from the figures that

$$\frac{n + \left(\frac{1}{2\beta}\right)}{n+1} \approx 1.0 \qquad (21)$$

$$\frac{n\beta + 1}{(n+1)\beta + 1} \approx \frac{n+2}{n+3} \qquad (22)$$

Therefore, equation (19) is reduced to

$$\Delta\widetilde{W}_C = \left[\frac{\sigma_{max}^2}{2\,\Delta\sigma}\right] \Delta\epsilon_e + \left(\frac{n+2}{n+3}\right) \left[\frac{f(n)}{2\pi}\right] \sigma_{max}\, \Delta\epsilon_C \qquad (23)$$

The crack propagation life relation, equations (18), (20), and (23), is independent of β and t_0. In other words, the life law is insensitive to the stress waveform as indicated in assumption (4).

Strainrange Partitioning (SRP) Life Relationships

Basic SRP Life Relationships

The SRP life relationships are derived based on the high-temperature fracture mechanics equations discussed in the previous section. The essential concepts of the SRP method for life prediction in high-temperature, low-cycle fatigue are given in reference 5. The framework of the method is summarized as follows. The inelastic strain range in a general creep-fatigue cycle may be comprised of components from as many as four basic types of strain ranges: $\Delta\epsilon_{PP}$, $\Delta\epsilon_{PC}$, and $\Delta\epsilon_{CP}$ or $\Delta\epsilon_{CC}$. Hysteresis loops of each type are illustrated in figure 1. They are referred to in shorthand notation as PP-, PC-, CP-, and CC-fatigue cycles. Each cycle type has a unique strain range versus life relationship formulated as follows:

$$\Delta\epsilon_{ij} N_{ij}^{m_{ij}} = D_{ij} \qquad (ij = PP,\ PC,\ CP, \text{ and } CC) \qquad (24)$$

where m_{ij} and D_{ij} are material constants, and $\Delta\epsilon_{ij}$ and N_{ij} are the inelastic strain range and the creep-fatigue cyclic life in ij fatigue. The life in a general creep-fatigue situation is

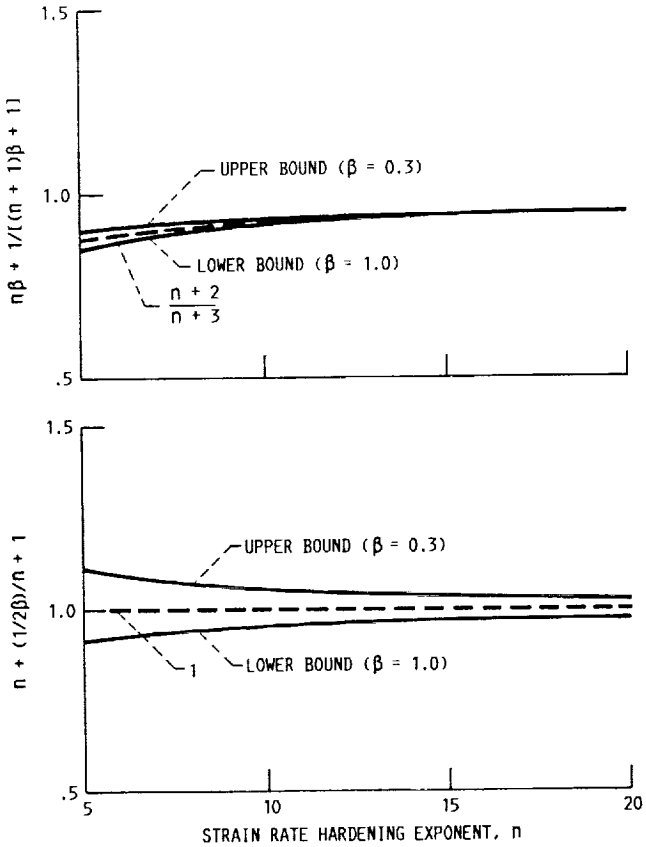

Figure 4.—Relations between terms in equation (19) and the strain rate hardening exponent n for β in the range of 0.3 to 1.0.

determined by the combination of the above life relationships through what is known as the Interaction Damage Rule (ref. 37)

$$\frac{1}{N_f} = \sum_{i,j} \left(\frac{\Delta\epsilon_{ij}}{\Delta\epsilon_{in}}\right)\left(\frac{1}{N_{ij}}\right) \tag{25}$$

where $\Delta\epsilon_{in}$ is the inelastic strain range.

The derivation of the basic SRP life relationships from the high-temperature fracture mechanics equations is as follows: For PP and PC fatigue, the following equations are derived from equations (5), (11), and (12):

PP-fatigue:

$$\left[\left(\frac{\Delta\sigma\ \Delta\epsilon_e}{2}\right) + \frac{f(n')}{2\pi}\ \Delta\sigma\ \Delta\epsilon_{PP}\right]^{m_f} N_{PP} = D_f(1 + \alpha_{PP}) \tag{26}$$

PC-fatigue:

$$\left[\left(\frac{\Delta\sigma\ \Delta\epsilon_e}{2}\right) + \frac{f(n')}{2\pi}\ \Delta\sigma\ \Delta\epsilon_{PC}\right]^{m_f} N_{PC} = D_f(1 + \alpha_{PC}) \tag{27}$$

Generally, α_{PP} is different from α_{PC}. For example, figure 5 shows the growth of surface cracks during high-temperature fatigue of 316 stainless steel at 977 K (ref. 38). Assuming that the crack initiates as the crack length reaches 0.1 mm, the initiation lives for PP and PC fatigue are given as in table I (from fig. 5). Strictly speaking, α is dependent on the strain range. However, for the sake of analytical simplicity we shall ignore this dependency (ref. 39). In low-cycle fatigue, the first terms in the left-hand side parentheses of equations (26) and (27) are negligible because $f(n')/2\pi$ is larger than 1/2 and $\Delta\epsilon_{PP}$ or $\Delta\epsilon_{PC}$ is much larger than $\Delta\epsilon_e$. Considering equation (7), equations (26) and (27) are reduced to

$$\Delta\epsilon_{PP}\overline{N_{PP}^{(n'+1)m_f}}^{n'} = \left\{\left[\frac{2\pi A^{1/n'}}{f(n')}\right]^{m_f} D_f(1 + \alpha_{PP})\right\}^{\overline{(n'+1)m_f}^{n'}} = D_{PP} \tag{28}$$

$$\Delta\epsilon_{PC}\overline{N_{PC}^{(n'+1)m_f}}^{n'} = \left\{\left[\frac{2\pi A^{1/n'}}{f(n')}\right]^{m_f} D_f(1 + \alpha_{PC})\right\}^{\overline{(n'+1)m_f}^{n'}} = D_{PC} \tag{29}$$

As the right-hand sides in the equations are constants, equations (28) and (29) coincide with the SRP life equations, equation (24).

For CC and CP fatigue, the following equations are derived from equations (5), (18), and (19)

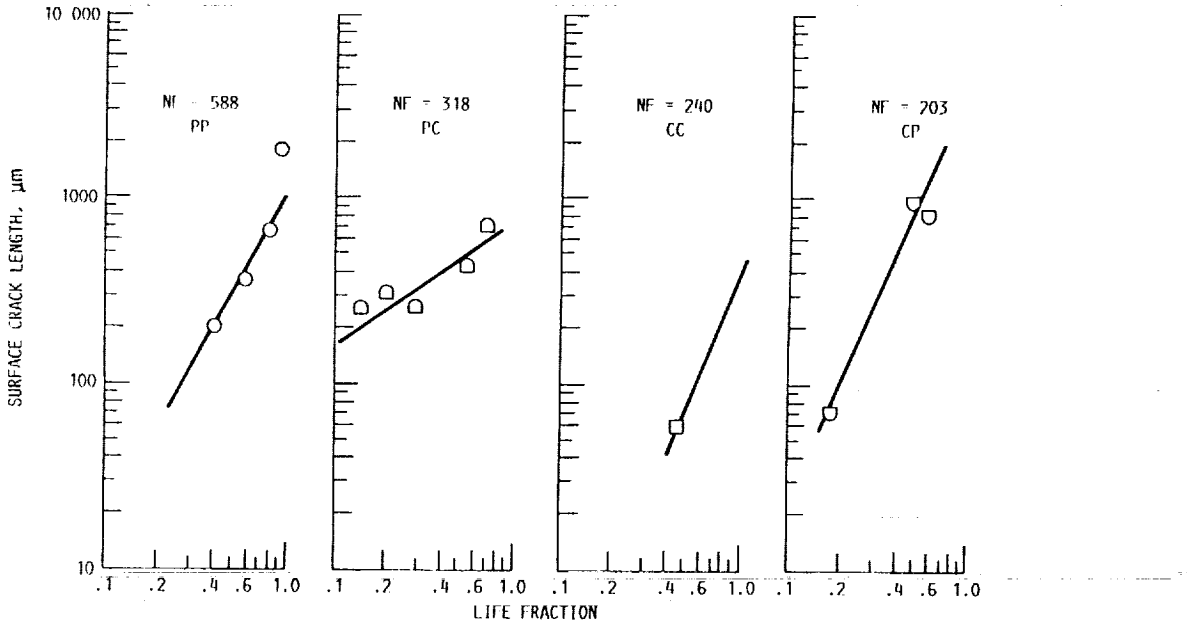

Figure 5.—Surface crack growth for SRP cycles, 316 stainless steel at 1300 °F.

TABLE I.—TYPICAL VALUES OF $\alpha = N_i/N_P$

Creep-fatigue cycle	Value of $\alpha = N_i/N_P$
PP	0.4
PC	<.1
CP	.3
CC	1.0

$$\left[\frac{n\beta+1}{(n+1)\beta+1}\right]\left[\frac{f(n)}{2\pi}\right]\sigma_{\max}\ \Delta\epsilon_{CP}N_{CP} = D_C(1+\alpha_{CP}) \tag{30}$$

$$\left[\frac{n\beta+1}{(n+1)\beta+1}\right]\left[\frac{f(n)}{2\pi}\right]\sigma_{\max}\ \Delta\epsilon_{CC}N_{CC} = D_C(1+\alpha_{CC}) \tag{31}$$

Here, the first term in equation (19) can be neglected for low-cycle fatigue. From equation (14) and (15), the relation between $\sigma_{\max}$ and $\Delta\epsilon_{CP}$ (or $\Delta\epsilon_{CC}$) is given as

$$\Delta\epsilon_{CP}\ (\text{or}\ \Delta\epsilon_{CC}) = \int_0^{t_0} B\sigma^n\,dt$$

$$= B\sigma_{\max}^n \int_0^{t_0}\left(\frac{t}{t_0}\right)^{\beta n} dt$$

$$= \left(\frac{Bt_0}{\beta n+1}\right)\sigma_{\max}^n \tag{32}$$

Substituting equation (32) into equations (30) and (31),

$$\Delta\epsilon_{CP}N_{CP}^{n/(n+1)} = \frac{[(n+1)\beta+1]^{n/(n+1)}}{n\beta+1}\,t_0^{1/(n+1)} \cdot B^{1/(n+1)}\left[\frac{2\pi}{f(n)}D_C(1+\alpha_{CP})\right]^{n/(n+1)} \tag{33}$$

$$\Delta\epsilon_{CC}N_{CC}^{n/(n+1)} = \frac{[(n+1)\beta+1]^{n/(n+1)}}{n\beta+1}\,t_0^{1/(n+1)} \cdot B^{1/(n+1)}\left[\frac{2\pi}{f(n)}D_C(1+\alpha_{CC})\right]^{n/(n+1)} \tag{34}$$

Equations (33) and (34) can be simplified by the following simplifying approximations. As shown in figure 6, $[(n+1)\beta + 1]^{n/n+1}/(n\beta+1)$ is approximately equal to unity in the range of $0 \le \beta \le 1.0$ and $5 \le n \le 20$.

Therefore, equations (33) and (34) are reduced to

$$\Delta\epsilon_{CP}N_{CP}^{n/(n+1)} = (Bt_0)^{1/(n+1)}\left[\frac{2\pi}{f(n)}D_C(1+\alpha_{CP})\right]^{n/(n+1)}$$

$$= D_{CP} \tag{35}$$

$$\Delta\epsilon_{CC}N_{CC}^{n/(n+1)} = (Bt_0)^{1/(n+1)}\left[\frac{2\pi}{f(n)}D_C(1+\alpha_{CC})\right]^{n/(n+1)}$$

$$= D_{CC} \tag{36}$$

Since $1/(n+1)$ is much smaller than unity, $t_0^{1/(n+1)}$ is nearly constant in usual experiments where t_0 exceeds less than about two orders of magnitude change. For example, in the case of $n = 10$, $t_0^{1/(n+1)}$ changes only 1.5 times as t_0 changes 100 times. Therefore, the right-hand sides in equations (35) and (36) are nearly constants. Equations (35) and (36) coincide with the SRP life relationships, equation (24).

Ductility-Normalized SRP Life Relationships

Modifying the basic SRP life relations by a creep or plastic ductility, material-independent SRP life equations called ductility-normalized life relations were proposed first by Manson (ref. 37) and then refined by Halford, Saltsman, and Hirschberg (ref. 40). The latter are written as follows:

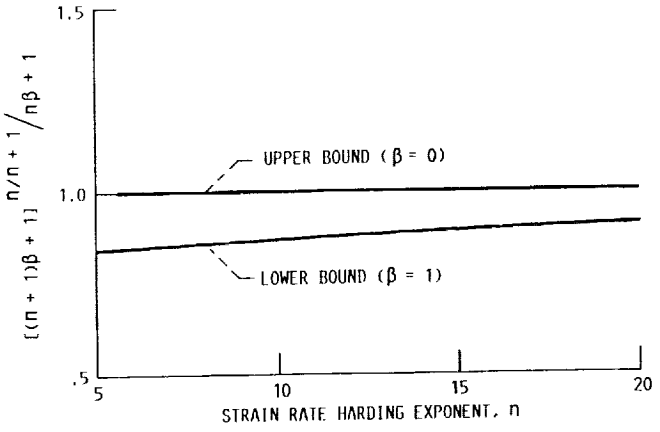

Figure 6.—Relations between terms in equations (33) and (34) and the strain rate hardening exponent n for β in the range of 0 to 1.0.

$$\Delta\epsilon_{PP}N_{PP}^{0.6} = 0.5\ \delta_P \tag{37}$$

$$\Delta\epsilon_{PC}N_{PC}^{0.6} = 0.25\ \delta_P \tag{38}$$

$$\Delta\epsilon_{CP}N_{CP}^{0.6} = 0.2\ \delta_C^{0.6} \quad (\text{or } 0.1\ \delta_C^{0.6}) \tag{39}$$

$$\Delta\epsilon_{CC}N_{CC}^{0.6} = 0.25\ \delta_C^{0.6} \tag{40}$$

where δ_P is tensile (plastic) ductility and δ_C is creep ductility. The key points in these life relations are (1) fatigue life is strongly dependent on the ductility and (2) the constants are essentially independent of material. In the following section, the effect of ductility on the life and the powers of the strain range versus life relations will be discussed.

Figures 7 and 8 show the fracture mechanics relations of several heat resisting alloys in CP and CC fatigue, and PP and PC fatigue, respectively (ref. 26). The data scatter for plots of $d\ell/dN - \Delta J_C$ for CP and CC fatigue is large, while for $d\ell/dN - \Delta J_f$ in PP and PC fatigue, the data scatter is considerably smaller. Figure 7 reveals that crack propagation rates of creep ductile materials (e.g., 0.16 percent C steel) are slower than that of creep-brittle materials (e.g., Hastelloy X) at a similar ΔJ_C. Then, $d\ell/dN$ is replotted against $\Delta J_C/\delta_C^{0.6}$ in figure 9.

Creep ductility values δ_C are as shown in figure 7. Independent of material,

$$\frac{d\ell}{dN} = 2.5\text{x}10^{-3}\left(\frac{\Delta J_C}{\delta_C^{0.6}}\right) \tag{41}$$

In other words, the material constant C_C in equation (3) (or eq. (2)) is proportional to $\delta_C^{0.6}$. Therefore, it is derived from equations (20), (35), and (36) that D_{CP} and D_{CC} are proportional to $\delta_C^{0.6}$. This corresponds with the ductility-normalized SRP life equations (eqs. (39) and (40) of Halford et al. (ref. 40)).

The dependence of crack growth rate on tensile plastic ductility is confirmed by figure 8. The seven alloys have about the same tensile plastic ductility δ_P, and they have about the same crack growth rates (ref. 26). Unfortunately, similar data are not available for low ductility alloys to confirm the generality of the relationship. If $d\ell/dN$ is proportional to $(\Delta J_f/\delta_P)^{mf}$ (by analogy to eq. (41)), $D_{PP} \propto (\delta_P)^{n'/(n'+1)mf}$ and $D_{PC} \propto (\delta_P)^{n'/(n'+1)mf}$ can be derived from equations (1),

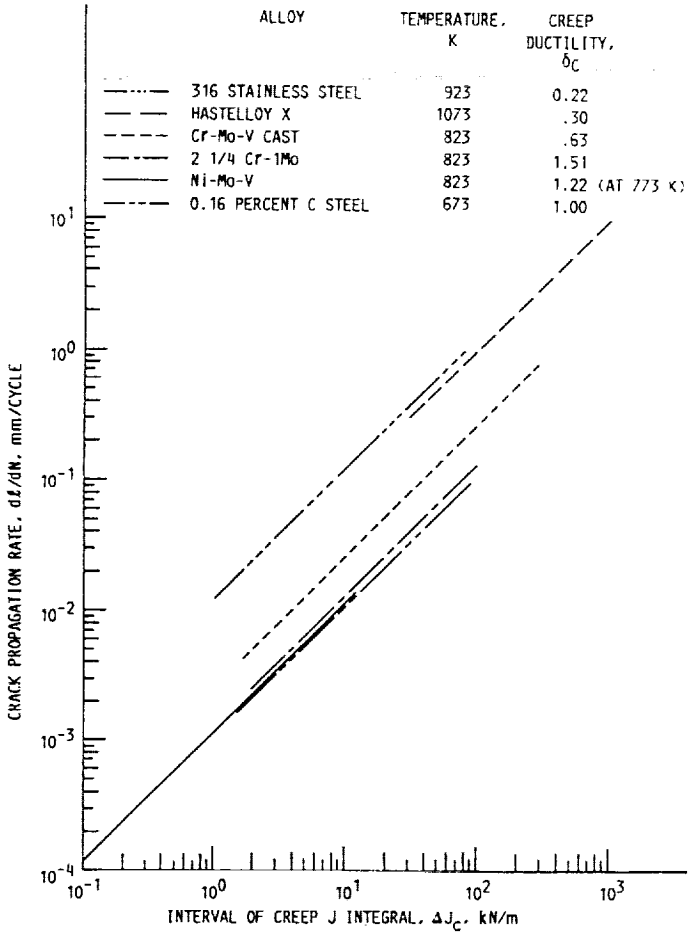

Figure 7.—Relation between crack propagation rate and interval of creep J integral in CP and CC fatigue for several high-temperature alloys.

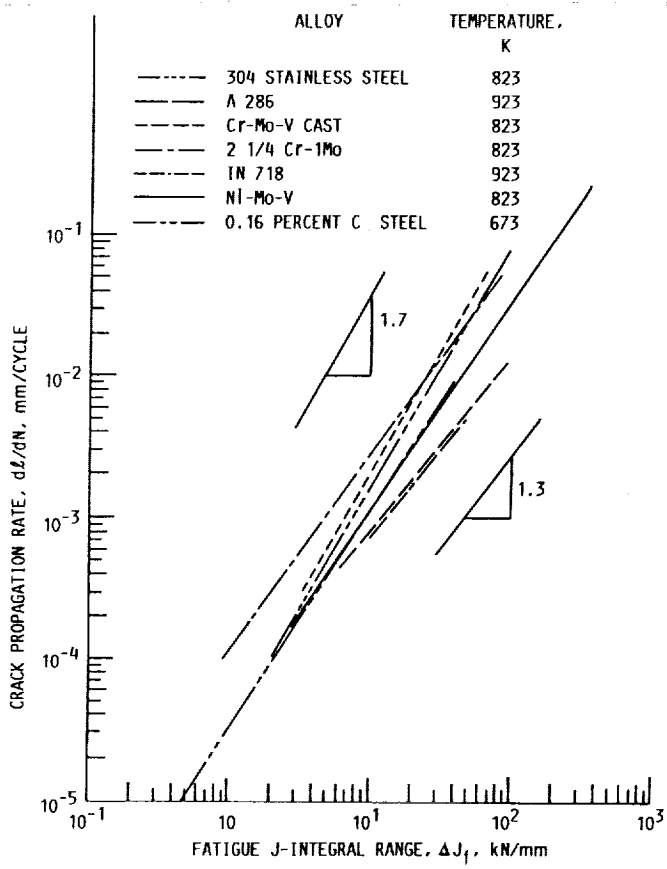

Figure 8.—Relation between crack propagation rate and fatigue J integral range in PP and PC fatigue for several high-temperature alloys.

(13), (28), and (29). Because $n'/(n' + 1)$ is nearly equal to 1.0 for $5 \leq n' \leq 15$, the ductility-normalized life relationships for PP and PC fatigue are derived. However, it should be noted that the relation between $d\ell/dN$ and $\Delta J_f/\delta_P$ must be verified by experiments (for materials with much different δ_P values).

From equations (28), (29), (35), and (36),

$$m_{PP} = m_{PC} = \frac{n'}{(n' + 1)m_f} \tag{42}$$

$$m_{CP} = m_{CC} = \frac{n}{n + 1} \tag{43}$$

where m_{ij} (ij = PP, PC, CP, and CC) is the power of the $\Delta\epsilon_{ij} - N_{ij}$ relation, equation (25). For engineering heat resisting alloys, n' and n are usually in the range $5 \leq n' \leq 15$, and $5 \leq n \leq 20$, respectively. Also, $1.3 \leq m_f \leq 1.7$ from figure 8. The ranges of values of m_{ij} calculated from equations (42) and (43) are listed in table II. They are observed to be close to the values of the exponents in the ductility-normalized SRP life relations as listed in table II.

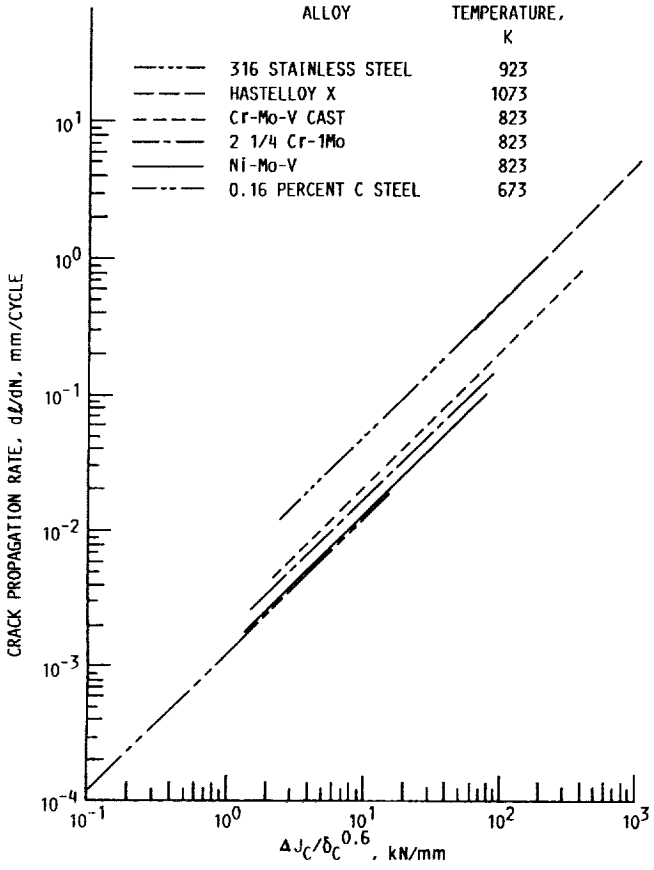

Figure 9.—Relation between crack propagation rate and ductility normalized interval of creep J integral in CP and CC fatigue for several high-temperature alloys.

TABLE II.—COMPARISON OF POWER m FOR CURRENT ANALYSIS AND DUCTILITY-NORMALIZED SRP EQUATIONS

Ducility-normalized SRP life relations	Power			
	m_{PP}	m_{PC}	m_{CP}	m_{CC}
Equations (42) and (43)	0.5 to 0.7	0.5 to 0.7	0.8 to 0.95	0.8 to 0.95
Halford et al. (ref. 40)	0.6	0.6	0.6	0.6
Manson et al. (ref. 37)	0.6	0.8	0.8	0.8

Thermal Fatigue SRP

References 41 and 42 report that the basic life relations, equation (24), at least for certain materials, are insensitive to temperature. In other words, m_{ij} and D_{ij} (ij = PP, PC, CP, and CC) are weak functions of temperature. This suggests the possibility of the direct applicability of isothermal SRP life relations to thermal fatigue life prediction for such alloys. The insensitivity of creep-fatigue behavior to isothermal temperature is discussed below.

Figures 10 and 11 show the dependence of the $d\ell/dN - \Delta J_f$, $d\ell/dN - \Delta J_C$ relations on temperature in PP and PC, and CP and CC fatigue, respectively for 304 stainless steel (ref. 43). Similar results have been obtained for several high-temperature alloys (ref. 43). From the figures, the constants, C_f, m_f, C_C, in the fracture mechanics relations (eqs. (1) and (3)) are insensitive to test temperature. This implies that D_C and D_P are insensitive to temperature as well by virtue of equations (13) and (20). Generally, n' and n are relatively insensitive to temperature, while A and B are quite temperature dependent. Therefore, in the life relations derived from fracture mechanics (eqs. (28), (29), (35), and (36)), the values of $(A)^{1/(n'+1)}$ and $(B)^{1/(n+1)}$ are mainly responsible for any temperature dependence. Because of the observation that $5 \leq n' \leq 15$, $5 \leq n \leq 20$, however, the dependence of $(A)^{1/(n'+1)}$ and $(B)^{1/(n+1)}$ on temperature is smaller than that of A and B alone. Figure 12 shows some examples of $(B)^{1/(n+1)}$ where B and n are obtained from steady state creep data (ref. 43). It thus can be concluded that m_{ij} and D_{ij} in the derived life relations are relatively insensitive to temperature for the alloys shown in figure 12.

Under thermomechanical fatigue (TMF) stress conditions the J integral and creep J integral need to be modified in order to retain their ability to represent the stress and strain singularity at a crack tip (ref. 44). For example, the $\hat{J}$ integral proposed by Kishimoto et al. (ref. 44) is one of the J integrals modified for such conditions, and is defined as

$$\hat{J} = \int_\Gamma \left(W_{eP}\, dx_1 - T_i u_{i,1}\, ds\right) + \int\int_a \xi\sigma_{ij}\left(\frac{\partial\Theta}{\partial x_1}\right)da \tag{44}$$

$$W_{eP} = \int_0^{\epsilon_{ij}^{eP}} \sigma_{ij}\, d\epsilon_{ij}^{eP} \tag{45}$$

where Γ, x_1, a, and ds are illustrated in figure 13, T_i is traction, u_i is displacement, ξ is the thermal expansion coefficient, σ_{ij} is stress, Θ is temperature, and ϵ_{ij}^{eP} is the mechanical elastic-plastic strain excluding thermal expansion. Under isothermal conditions $\hat{J}$ reduces to J and retains its physical meaning during TMF. The term J^* is also modified by referring to the $\hat{J}$ integral as follows:

$$\hat{J}^* = \int_\Gamma \left(W_i^*\, dx_1 - T_i \dot{u}_{i,1}\, ds\right) + \int\int_a \xi \sigma_{ij} \left(\frac{\partial \dot{\Theta}}{\partial x_1}\right) da \tag{46}$$

$$W_i^* = \int_0^{\dot{\epsilon}^C} \sigma_{ij}\, d\dot{\epsilon}_{ij}^C \tag{47}$$

where $\dot{\epsilon}_{ij}^C$ is creep strain rate (dot indicates time derivative).

The definition of ΔJ_f and ΔJ_C in TMF is extended on the basis of the $\hat{J}$ and $\hat{J}^*$ integrals;

$$\Delta J_f = \hat{J}_{\max} - \hat{J}_{\min} \tag{48}$$

$$\Delta J_C = \int_0^{t_0} \hat{J}^*\, dt \tag{49}$$

where $\hat{J}_{\max}$ and $\hat{J}_{\min}$ are the maximum and minimum values of J integral in a cycle, respectively. In TMF, as well as isothermal fatigue, it has been shown (ref. 45) that the crack propagation rate $d\ell/dN$ correlates well with ΔJ_f or ΔJ_C. Repeating equations (1) and (2) gives

$$\frac{d\ell}{dN} = C_f\, \Delta J_f^{\,m_f}$$

for time-independent cycling (i.e., PP and PC fatigue) and

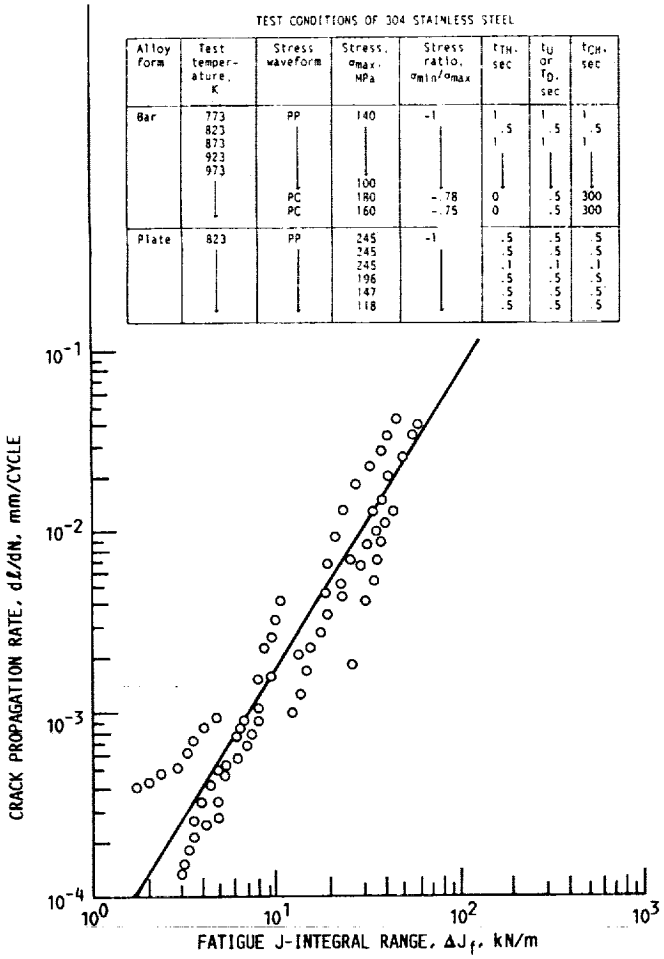

Figure 10.—Weak temperature dependence of crack propagation rate on the fatigue J-integral range (from ref. 43).

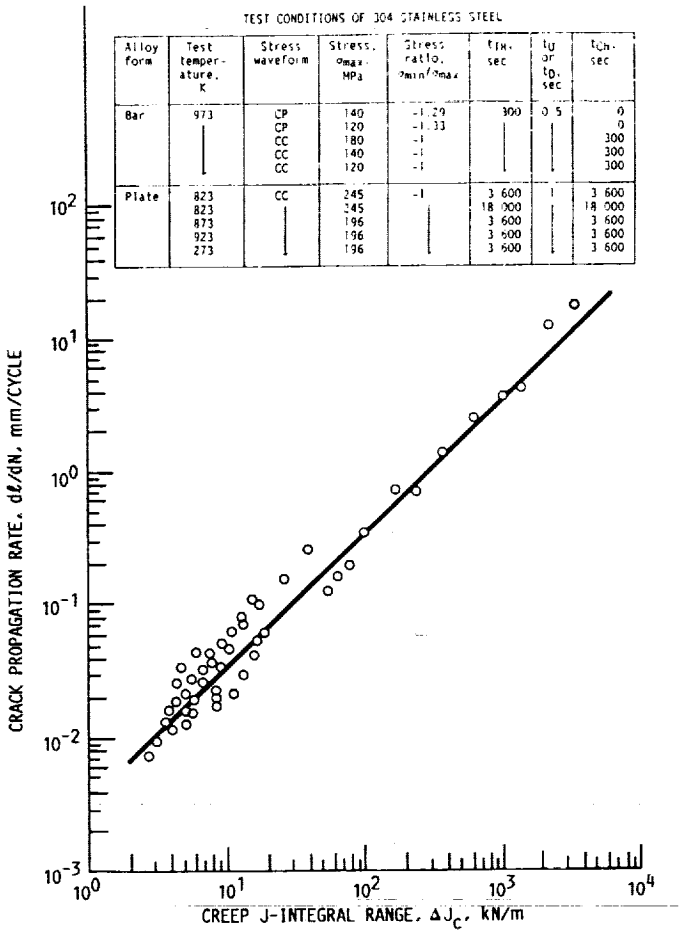

Figure 11.—Weak temperature dependence of crack propagation rate on the interval of creep J integral (from ref. 43).

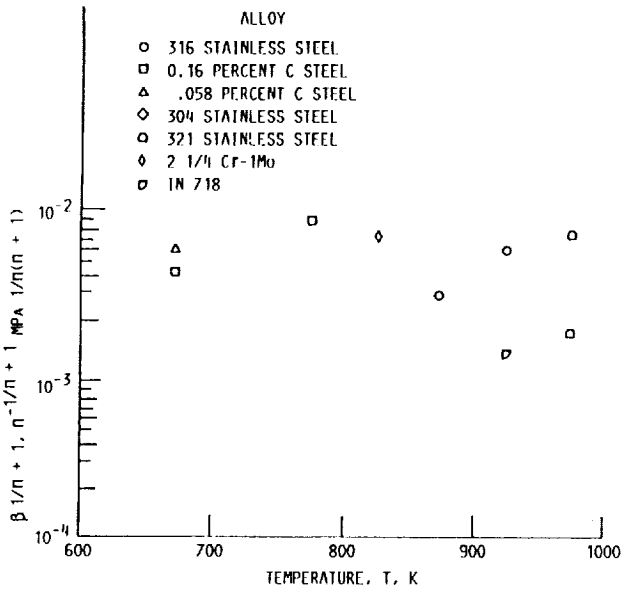

Figure 12.—Weak temperature dependence of $(B)^{1/(n+1)}$.

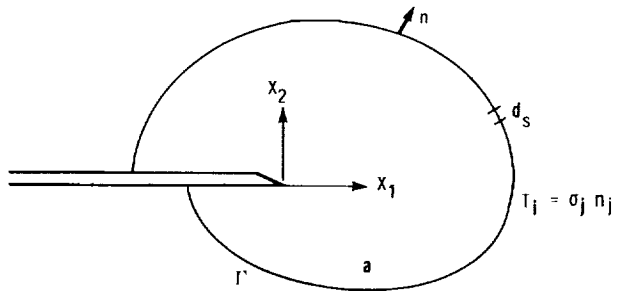

Figure 13.—Crack tip coordinates and area of integral path. (Here n_j is a component of n, the normal vector to the path Γ.)

$$\frac{d\ell}{dN} = C_C\,\Delta J_C$$

for time-dependent cycling (i.e., CP and CC fatigue). With the assumption that only A is dependent on temperature, the effect of temperature change on the derived life relations, equations (35) and (36), is caused principally by $(A)^{1/(n'+1)}$. However, the temperature effect is small and thus the life relations in PP and PC fatigue under TMF are similar to those under isothermal conditions. However, it is extremely difficult to prove that the life relations in CC and CP fatigue under TMF are similar to those under isothermal fatigue because ΔJ_C cannot be formulated as a simple form of equation (17). The first author obtained similar life relations for both in-phase TMF and isothermal fatigue, but this work is as yet unpublished. In the analysis summarized below, in-phase TMF conditions are assumed (tension at high temperature and compression at low temperature). Also assumed are the following relations:

$$\dot{\epsilon}_C = B'\exp\left(\frac{-Q}{R\Theta}\right)\sigma^n \tag{50}$$

$$\Theta = kt^{\gamma} + \Theta_0 \qquad \left(\Theta_{\max} = kt_0^{\gamma} + \Theta_0\right) \tag{51}$$

$$\sigma = \sigma_{\max}\left(\frac{t}{t_0}\right)^{\beta} \tag{15}$$

where B', Q, R, k, γ, $\Theta_{\max}$, and Θ_0 are constants, and Θ is temperature. From these equations and equation (2)

$$N_{Pg}\,\Delta\widetilde{W}_C = D_C \tag{52}$$

and

$$\Delta\widetilde{W}_C = \left(\frac{n+2}{n+3}\right)\left[\frac{f(n)}{2\pi}\right]\sigma_{\max}\,\Delta\epsilon_C \tag{53}$$

where $g\,\Delta\widetilde{W}_C$ is the hysteretic energy in TMF cycling. This has the same form as equation (18) in isothermal fatigue provided g is a constant near unity. It is recognized that $g\,\Delta\widetilde{W}_C$ is different from $\Delta\widetilde{W}_C$ in isothermal fatigue (eq. (23)). A numerical integral must be derived in order to evaluate g in in-phase TMF. Such an integral is given below

$$g = \left(\frac{n+3}{n+2}\right)\left[\frac{1}{(\Theta_{\max}-\Theta_0)^{\beta/\gamma}}\right] \cdot \frac{\displaystyle\int_{\Theta_0}^{\Theta_{\max}} \exp\left(\frac{-Q}{R\Theta}\right)(\Theta-\Theta_0)^{\frac{\beta(n+1)-\gamma+1}{\gamma}}\,d\Theta}{\displaystyle\int_{\Theta_0}^{\Theta_{\max}} \exp\left(\frac{-Q}{R\Theta}\right)(\Theta-\Theta_0)^{\frac{\beta n-\gamma+1}{\gamma}}\,d\Theta} \tag{54}$$

Figure 14 shows the ratio g for several values of n, β, γ, and $Q/R\Theta_0$. Here, $\Theta_{\max}$ and Θ_0 are the maximum temperature and temperature at $t = 0$, respectively. An evaluation of g was made for conditions covering a practical range of fatigue conditions for high temperature alloys (i.e., $10 \le Q/R_0 \le 250$, $1.0 \le \Theta_{\max}/\Theta_0 \le 3$, $0.3 \le \gamma \le 3.0$, $0.3 \le \beta \le 1.0$, $5 \le n \le 20$). As a result, g was between 0.97 and 1.15 for all conditions examined. This implies that

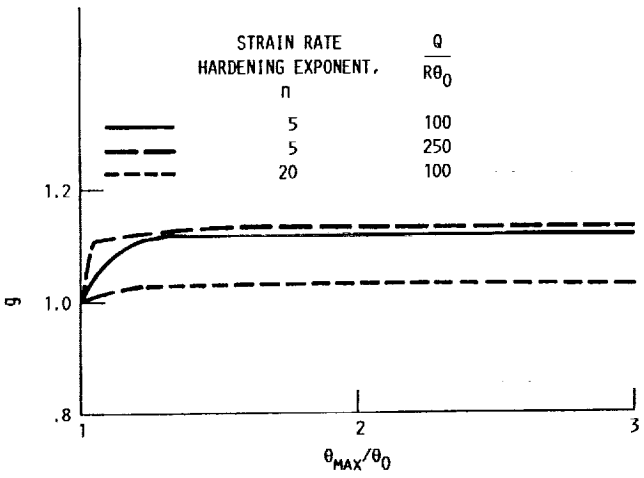

Figure 14.—Several examples of the influence of (Θ_{max}/Θ_0) on equation (54) for values of n, β, γ, and $Q/R\Theta_0$ ($\beta = 0.5$ and $\gamma = 1.0$).

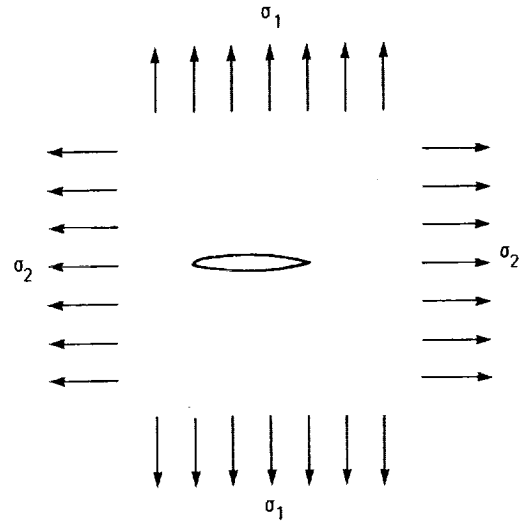

Figure 15.—Crack under remote biaxial stress conditions.

the same law governs the lives in both TMF and isothermal fatigue for the conditions considered herein.

Future Considerations—Multiaxiality

It is expected that there are also links between SRP and fracture mechanics principals for multiaxial loading conditions. However, nonlinear, time- and temperature-dependent fracture mechanics analyses (ref. 46) and SRP analyses (refs. 11 and 12) for multiaxial stress states are in their infancy. In addressing issues specific to SRP that are associated with cyclic multiaxial stress-strain states, Manson and Halford (ref. 11) have proposed preliminary rules for dealing with dominant directions of stress and strain during proportional loadings. Directionality of loading is of utmost importance in establishing the orientation of creep-fatigue crack growth, and in establishing the directions of creep and plasticity reversal. Identical considerations are also unavoidable in applying fracture mechanics concepts to high-temperature creep-fatigue crack propagation. However, even if a crack propagates in Mode I under biaxial stress conditions as shown in figure 15, the value of J^* is strongly dependent on not only the normal stress σ_1 but also the lateral stress σ_2 (ref. 47). Therefore, equations (8) and (16) would have to be modified to include the effects of both stresses. Such equations have as yet to be established. Moreover, high temperature multiaxial fracture mechanics, especially for modes other than Mode I is still in a virtually undeveloped stage. This remains an area of fertile, future research activity.

Future Considerations—Nominally Elastic Creep-Fatigue

The classical version of SRP concentrated on using the inelastic strain range as the primary life controlling parameter for creep-fatigue analysis. Analysts performing engineering life predictions in the practical low-total strain, long-life, nominally elastic regime, however, avoided use of the SRP approach because of the inherent difficulties in accurately calculating very small quantities of inelasticity in a complex structural component. Recently, however, the total strain version of SRP (TS-SRP) (refs. 15, 20, and 21) has been developed to circumvent these practical difficulties wherein the elastic strain range dominates the contributions to the total strain range. The TS-SRP approach is also applicable to the life prediction of high strength superalloys that exhibit high-total strains with accompanying low-inelastic strains. In the low-total strain regime, the crack initiation process dominates the life. Thus it is unrealistic to derive the life equations solely from fracture mechanics (i.e., crack growth) concepts. However, it is expected that in the high-total strain, low-inelastic regime of superalloys, consideration based on fracture mechanics concepts is directly applicable if crack propagation plays a dominant role in the failure process. For this case the following equation is derived from equations (12) and (19) taking into consideration both the first and second terms:

$$\left(C_i\,\Delta\epsilon_e^2 + C'\,\Delta\epsilon_{ij}^{\bar{n}}\right)N_{ij}^{1/\bar{m}} = D_{ij} \qquad (55)$$

where,

$$\bar{n} = \frac{n'}{n'+1},\ \bar{m} = \frac{1}{m_f} \qquad \text{for } ij = PP \text{ and } PC$$

$$\bar{n} = \frac{n}{n+1},\ \bar{m} = 1.0 \qquad \text{for } ij = CP \text{ and } CC$$

This has a form similar to that of TS-SRP, although the detail is different. As experimental data are insufficient to verify the validity of applying fracture mechanics concepts to these conditions, further discussion must be deferred to the future.

Summary of Results

Links have been established between the description of high-temperature creep-fatigue behavior of engineering alloys by the methods of Strainrange Partitioning and those based on nonlinear, high-temperature fracture mechanics principals. These are summarized as follows:

1. The basic SRP inelastic strain range versus cyclic life relationships have been derived from high-temperature, nonlinear, fracture mechanics considerations. The derived SRP life relationships are in reasonable agreement with experience on the SRP behavior of many high-temperature alloys.

2. Fracture mechanics have served as a basis for the derivation of the ductility-normalized SRP life relationships.

3. Thermal fatigue SRP life prediction equations based on high-temperature, nonlinear fracture mechanics have been derived.

4. Areas of future exploration of links between fracture mechanics and SRP have been identified for multiaxial loading and low-strain, long-life, nominally elastic conditions.

National Aeronautics and Space Administration
Lewis Research Center
Cleveland, Ohio, April 14, 1989

References

1. Coffin, L.F., Jr., et al.: Time-Dependent Fatigue of Structural Alloys. A General Assessment(1975). ORNL 5073, Oak Ridge National Laboratories, 1977.
2. Solomon, H.D., et al., eds: Low Cycle Fatigue, ASTM-STP-942, American Society for Testing and Materials, Philadelphia, 1988.
3. Halford, G.R.: Low-Cycle Thermal Fatigue. Chapter 6, Thermal Stresses II, R.B. Hetnarski, ed., Elsevier Science Publishers B.V., Amsterdam, 1987, pp. 329-428.
4. Ohtani, R.; Ohnami, M.; and Inoue, T.; eds.: High Temperature Creep-Fatigue. Current Japanese Materials Research. Vol. 3, Elsevier Applied Science Publishers Ltd., 1988.
5. Manson, S.S.; Halford, G.P.; and Hirschberg, M. H.: Creep-Fatigue Analysis by Strain-Range Partitioning. Design for Elevated Temperature Environment, S.Y. Zamrik, ed., ASME, 1971, pp. 12-24.
6. Characterization of Low Cycle High Temperature Fatigue by the Strainrange Partitioning Method. AGARD CP-243, Advisory Group Aerospace Research and Development, Paris, France, 1978. (Avail. NTIS, AD-A059900).
7. Kinner, W.K.: Strainrange Partitioning. Mater. Eng., vol. 89, no. 6, June 1979, pp. 41-43.
8. Hirakawa, K.; and Tokimasa, K.: Effect of Environment on Partitioned Strain-Life Relations $\Delta\epsilon_{ij}$–N_{ij} of SUS 304 Stainless Steel. J. Soc. Mater. Sci., Jpn. (In Japanese), vol. 28, no. 308, May 1979, pp. 386-392.
9. Report of Colaboratral Work on Creep-Fatigue Test. Low Cycle Fatigue Behavior of 18Cr−8Ni Steel at High Temperature Based on Strainrange Partitioning Method (In Japanese), 1981.
10. Vogel, W.H.; Soderquist, R.W.; and Schlein, B.C.: Application of Creep-LCF Cracking Model to Combustor Durability Prediction. Fatigue Life Technology, T.A. Cruse and J.P. Gallagher, eds., ASME, 1977, pp. 23-31.
11. Manson, S.S.; and Halford, G.R.: Treatment of Multiaxial Creep-Fatigue by Strainrange Partitioning. 1976 ASME-MPC Symposium on Creep-Fatigue Interaction, R.M. Curran, ed., ASME, 1976, pp. 299-322.
12. Manson, S.S.; and Halford, G.R.: Discussion to paper by J.J. Blass and S. Y. Zamrik, "Multiaxial Low-Cycle Fatigue of Type 304 Stainless Steel," 1976 ASME-MPC Symposium on Creep-Fatigue Interaction, ASME, 1976, pp. 129-159. J. Eng. Mater. Technol., vol. 99, no. 3, July 1977, pp. 283-286.
13. Manson, S.S.; and Halford, G.R.: Complexities of High Temperature Metal Fatigue −Some Steps Toward Understanding. Israel J. Tech., vol. 21, no. 1-2, 1983, pp. 29-53. (NASA TM-83507).
14. Halford, G.R.; and Manson, S.S.: Life Prediction of Thermal-Mechanical Fatigue Using Strainrange Partitioning. Thermal Fatigue of Materials and Components, ASTM-STP-612, D.A. Spera and D.F. Mowbray, eds., American Society for Testing and Materials, 1976, pp. 239-254.
15. Saltsman, J.F.; and Halford, G.R.: Life Prediction of Thermomechanical Fatigue Using Total Strain Version of Strainrange Partitioning (SRP)—A Proposal. NASA TP-2779, 1988.
16. Thakker, A.B.; and Cowles, B.A.: Low Strain, Long Life Creep Fatigue of AF2-IDA and INCO 718. (FR-15652, Pratt and Whitney Aircraft Group; NASA Contract NAS3-22387), NASA CR-167989, 1983.
17. Manson, S.S.; and Zab, P.: A Framework for Estimation of Environmental Effect in High Temperature Fatigue. Environmental Degradation of Engineering Materials, Virginia Tech Printing Dept., Virginia Polytechnic Institute, Blacksburg, VA, 1977, pp. 757-770.
18. Kalluri, S.; Manson, S.S.; and Halford, G. R.: Exposure Time Considerations in High Temperature Low Cycle Fatigue. Mechanical Behavior of Materials-V (ICM-5), Vol. 2, M.G. Yan, S.H. Zhang, and Z.M. Zheng, eds., Pergamon Press, 1987, pp. 1029-1036.
19. Kalluri, S.; Manson, S.S.; and Halford, G.R.: Environmental Degradation of 316 Stainless steel in High Temperature Low Cycle Fatigue. Environmental Degradation of Engineering Materials III, M.R. Louthan Jr., R.P. McNitt, and R.D. Sisson Jr., eds., The Pennsylvania State University, University Park, PA, 1987, pp. 503-519.
20. Halford, G.R.; and Saltsman, J.F.: Strainrange Partitioning−A Total Strainrange Version. Advances in Life Prediction Methods, D.A. Woodford and J.R. Whitehead, eds., ASME, 1983, pp. 17-26.
21. Saltsman, J.F.; and Halford, G.R.: An Update of the Total Strain Version of Strainrange Partioning. Low Cycle Fatigue, ASTM-STP-942, H. D. Solomon, et al., eds., American Society for Testing and Materials, Philadelphia, 1988, pp. 329-341.
22. Manson, S.S.; and Halford, G.R.: Relation of Cyclic Loading Pattern to Microstructural Fracture in Creep-Fatigue. Fatigue 84, Vol. 3, C.J. Beevers, ed., Engineering Materials Advisory Services, Ltd., Warley, England, 1984, pp. 1237-1255.

23. Taira, S.; Fujino, M; and Yoshida, M.: Grain Boundary Sliding in Isothermal and Thermal Fatigue of 304 Stainless Steel. J.Soc. Mater. Sci., Jpn. (In Japanese), vol. 27, no. 296, May 1978, pp. 447-453.
24. Ohtani, R.; Kinami, T.; and Sakamoto, H.: Small Crack Propagation in High Temperature Creep-Fatigue of 304 Stainless Steel. Trans. JSME, vol. 52-A, no. 480, Aug. 1986, pp. 1824-1830.
25. Ohtani, R., et al.: High-Temperature Low-Cycle Fatigue Crack Propagation and Life Laws of Smooth Specimens Derived from the Crack Propagation Laws. Low Cycle Fatigue, ASTM-STP-942, H.D. Solomon, G.R. Halford, L.R. Kaisand, and B. N. Leis, eds., American Society for Testing and Materials, Philadelphia, 1988, pp. 1163-1180.
26. Ohtani, R.; and Kitamura, T.: Characterization of High-Temperature Strength of Metals Based on Mechanics of Crack Propagation. High Temperature Creep Fatigue, Current Japanese Materials Research, Vol. 3, R. Ohtani, M. Ohnami, and T. Inoue, eds., Elsevier Applied Science Publishers, Ltd., 1988, pp. 65-90.
27. Hirschberg, M.H.; and Halford, G.R.: Use of Strainrange Partitioning to Predict High-Temperature Low-Cycle Fatigue Life. NASA TN D-8072, 1976.
28. Dowling, N.E.; and Begley, J.A.: Fatigue Crack Growth During Gross Plasticity and the J Integral. Scientific Paper 74-1E7-CREEP-P1, Westinghouse Research Laboratories, Pittsburgh, PA, 1974.
29. Landes, J.D.; and Begley, J.A.: A Fracture Mechanics Approach to Creep Crack Growth. Mechanics of Crack Growth, ASTM-STP-590, American Society for Testing and Materials, 1976, pp. 128-148.
30. Saxena, A.: Evaluation of C* for the Characterization of Creep-Crack-Growth Behavior in 304 Stainless Steel. Fracture Mechanics, ASTM-STP-700, J.B. Wheeler, ed., American Society for Testing and Materials, 1980, pp. 131-151.
31. Ohji, K.; and Kubo, S.: Fracture Mechanics Evaluation of Crack Growth Behavior Under Creep and Creep-Fatigue Conditions. High Temperature Creep Fatigue, Current Japanese Materials Research, Vol. 3, R. Ohtani, M. Ohnami, and T. Inoue, eds., Elsevier Applied Science Publishers, Ltd., 1988, pp. 91-113.
32. Dowling, N.E.: J-Integral Estimates for Cracks in Infinite Bodies. Eng. Fract. Mech., vol. 26, no. 3, 1987, pp. 333-348.
33. He, M.Y.; and Hutchinson, J.W.: The Penny-Shaped Crack and the Plane Strain Crack in an Infinite Body of Power-Law Material. J. Appl. Mech., vol. 48, no. 4, Dec. 1981, pp. 830-840.
34. Mowbray, D.F.: Derivation of a Low-Cycle Fatigue Relationship Employing the J-Integral Approach to Crack Growth. Cracks and Fracture, ASTM-STP-601, J.L. Swedlow and M.L. Williams, eds., American Society for Testing and Materials, 1976, pp. 33-46.
35. Ohtani, R.: Stress and Strain Concentrations of Notched Members in Creep. J. Mater. Sci., Jpn. (In Japanese), vol. 25, no. 270, Mar. 1976, pp. 230-235.
36. Ohtani, R.; and Kitamura, T.: On the Fatigue Life Law for Smooth Specimens at Elevated Temperature Derived from the Fracture Mechanics Laws of Crack Propagation. J. Soc. Mater. Sci. Jpn. (In Japanese), vol. 34, no. 382, July 1985, pp. 843-849.
37. Manson, S.S.: The Challenge to Unify Treatment of High Temperature Fatigue—A Partisan Proposal Based on Strainrange Partitioning. Fatigue at Elevated Temperatures, ASTM-STP-520, A.E. Carden, A.J. McEvily, and C.H. Wells, eds., American Society for Testing and Materials, Philadelphia, 1973, pp. 744-782.
38. Manson, S.S; Halford, G.R.; and Oldrieve, R.E.: Relation of Cyclic Loading Pattern to Microstructural Fracture in Creep-Fatigue. NASA TM-83473, 1983.
39. Usami, S.; Fukuda, Y.; and Shida, S.: Micro-Crack Initiation and Propagation in 304 Stainless Steel Plain Specimen Under Fatigue-Oxidation Interaction at Elevated Temperature. J. Mater. Sci. Jpn. (In Japanese), vol. 33, no. 369, June 1984, pp. 685-691.
40. Halford, G.R.; Saltsman, J.F.; and Hirschberg, M.H.: Ductility Normalized-Strainrange Partitioning Life Relations for Creep-Fatigue Life Predictions. Environmental Degradation of Engineering Materials, Virginia Tech. Printing Dept., Virginia Polytechnic Institute, Blacksburg, VA, 1977, pp. 599-612.
41. Halford, G.R.; Hirschberg, M.H.; and Manson, S.S.: Temperature Effects on the Strainrange Partitioning Approach for Creep-Fatigue Analysis. Fatigue at Elevated Temperatures, ASTM-STP-520, A.E. Carden, A.J. McEvily, and C.H. Wells, eds., American Society for Testing and Materials, Philadelphia, 1973, pp. 658-669.
42. Halford, G.R.; and Manson, S.S.: Life Prediction of Thermal-Mechanical Fatigue Using Strainrange Partitioning. Thermal Fatigue of Materials and Components, ASTM-STP-612, D.A. Spera and D.F. Mowbray, eds., American Society for Testing and Materials, 1976, pp. 239-254.
43. Kitamura, T.: Study on Crack Propagation in High Temperature Fatigue Based on Fracture Mechanics. Doctoral Dissertation, Kyoto University (In Japanese), 1986.
44. Kishimoto, K.; Aoki, S.; and Sakata, M.: On the Path Independence Integral-J. Eng. Fract. Mech., vol. 13, no. 4, 1980, pp. 841-850.
45. Ohtani, R.; Kitamura, T.; and Tada, N.: Crack Propagation of Varying-Temperature Low-Cycle Fatigue Simulating Thermal Fatigue. Mechanical Behavior of Materials-V(ICM-5), Vol. 2, M.G. Yan, S.H. Zhang, and Z.M. Zheng, eds., Pergamon Press, 1987, pp. 1101-1108.
46. Sakane, M.; Ohnami, M.; and Sawada, M.: Fracture Modes and Low Cycle Biaxial Fatigue Life at Elevated Temperature. J. Eng. Mater.Technol., vol. 109, no. 3, July 1987, pp. 236-243.
47. Jansson, S.: Creep Crack Growth in Austenitic Stainless Steel Under Biaxial Loading. Proceedings of the International Conference on Creep, Japan Society of Mechanical Engineers, Tokyo, Japan, 1986, pp. 155-160.

NASA
National Aeronautics and Space Administration

Report Documentation Page

1. Report No.	2. Government Accession No.	3. Recipient's Catalog No.
NASA TM-4133		

4. Title and Subtitle

A Nonlinear High Temperature Fracture Mechanics Basis for Strainrange Partitioning

5. Report Date

October 1989

6. Performing Organization Code

7. Author(s)

Takayuki Kitamura and Gary R. Halford

8. Performing Organization Report No.

E-4733

10. Work Unit No.

553-13-00

9. Performing Organization Name and Address

National Aeronautics and Space Administration
Lewis Research Center
Cleveland, Ohio 44135-3191

11. Contract or Grant No.

13. Type of Report and Period Covered

Technical Memorandum

12. Sponsoring Agency Name and Address

National Aeronautics and Space Administration
Washington, D.C. 20546-0001

14. Sponsoring Agency Code

15. Supplementary Notes

Takayuki Kitamura, National Research Council—NASA Research Associate; present address: Department of Engineering Science, Kyoto University, Kyoto, Japan. Gary R. Halford, NASA Lewis Research Center.

16. Abstract

A direct link has been established between Strainrange Partitioning (SRP) and high-temperature fracture mechanics by deriving the general SRP inelastic strain range versus cyclic life relationships from high-temperature, nonlinear, fracture mechanics considerations. The derived SRP life relationships are in reasonable agreement based on the experience of the SRP behavior of many high-temperature alloys. In addition, fracture mechanics has served as a basis for derivation of the Ductility-Normalized SRP life equations, as well as for examination of SRP relations that are applicable to thermal fatigue life prediction. Areas of additional links between nonlinear fracture mechanics and SRP have been identified for future exploration. These include effects of multiaxiality as well as low-strain, nominally elastic, long-life creep-fatigue interaction.

17. Key Words (Suggested by Author(s))	18. Distribution Statement
Fracture mechanics; Crack growth; Fatigue (metal); Creep-fatigue; Strainrange partitioning; Creep crack growth; J-integral; Life prediction	Unclassified – Unlimited Subject Category 39

19. Security Classif. (of this report)	20. Security Classif. (of this page)	21. No of pages	22. Price*
Unclassified	Unclassified	20	A03

NASA FORM 1626 OCT 86

*For sale by the National Technical Information Service, Springfield, Virginia 22161

NASA-Langley, 1989